Formation of a Thymine-Hg II -Thymine Metal-Mediated DNA Base Pair: Proposal and Theoretical Calculation of the Reaction Pathway

7 AUTHORS, INCLUDING:

Jakub Sebera
Academy of Sciences of the Czech Republic
38 PUBLICATIONS   337 CITATIONS

SEE PROFILE

Michal Straka
Academy of Sciences of the Czech Republic
62 PUBLICATIONS   1,020 CITATIONS

SEE PROFILE

Ono Akira
Kanagawa University
137 PUBLICATIONS   2,844 CITATIONS

SEE PROFILE

Yoshiyuki Tanaka
Tokushima Bunri University
80 PUBLICATIONS   2,013 CITATIONS

SEE PROFILE

Formation of a Thymine-Hg^II-Thymine Metal-Mediated DNA Base Pair: Proposal and Theoretical Calculation of the Reaction Pathway

Jakub Šebera,[a, f] Jaroslav Burda,[b] Michal Straka,[a] Akira Ono,[c] Chojiro Kojima,[d] Yoshiyuki Tanaka,[e] and Vladimír Sychrovský*[a]

Abstract: A reaction mechanism that describes the substitution of two imino protons in a thymine:thymine (T:T) mismatched DNA base pair with a Hg^II ion, which results in the formation of a (T)N3-Hg^II-N3(T) metal-mediated base pair was proposed and calculated. The mechanism assumes two key steps: The formation of the first Hg^II–N3(T) bond is triggered by deprotonation of the imino N3 atom in thymine with a hydroxo ligand on the Hg^II ion. The formation of the second Hg^II–N3(T) bond proceeds through water-assisted tautomerization of the remaining, metal-nonbonded thymine base or through thymine deprotonation with a hydroxo ligand of the Hg^II ion already coordinated to the thymine base. The thermodynamic parameters $\Delta G_R = -9.5$ kcal mol^{-1}, $\Delta H_R = -4.7$ kcal mol^{-1}, and $\Delta S_R = 16.0$ cal mol^{-1}K^{-1} calculated with the ONIOM (B3LYP:BP86) method for the reaction agreed well with the isothermal titration calorimetric (ITC) measurements by Torigoe et al. [H. Torigoe, A. Ono, T. Kozasa, *Chem.*

Eur. J. **2010**, *16*, 13218–13225]. The peculiar positive reaction entropy measured previously was due to both dehydration of the metal and the change in chemical bonding. The mercury reactant in the theoretical model contained one hydroxo ligand in accord with the experimental pK_a value of 3.6 known for an aqua ligand of a Hg^II center. The chemical modification of T:T mismatched to the T-Hg^II-T metal-mediated base pair was modeled for the middle base pair within a trinucleotide B-DNA duplex, which ensured complete dehydration of the Hg^II ion during the reaction.

Keywords: DNA structures · mercury · metalation · metal–DNA binding · nucleobases

[a] Dr. J. Šebera, Dr. M. Straka, Dr. V. Sychrovský
Present address: Department of Molecular Spectroscopy
Institute of Organic Chemistry and Biochemistry, v.v.i.
Academy of Sciences of the Czech Republic
Flemingovo náměstí 2, 16610, Prague (Czech Republic)
E-mail: vladimir.sychrovsky@uochb.cas.cz

[b] Prof. J. Burda
Department of Chemical Physics and Optics
Faculty of Mathematics and Physics
Charles University in Prague
Ke Karlovu 3, 12116 Prague (Czech Republic)

[c] Prof. A. Ono
Department of Material & Life Chemistry
Faculty of Engineering, Kanagawa University
3-27-1 Rokkakubashi, Kanagawa, Yokohama
Kanagawa-ken 221-8686 (Japan)

[d] Prof. C. Kojima
Institute for Protein Research, Osaka University
3-2 Yamadaoka, Suita, Osaka 565-0871 (Japan)

[e] Prof. Y. Tanaka
Laboratory of Molecular Transformation
Graduate School of Pharmaceutical Sciences, Tohoku University
6-3 Aza-Aoba, Aramaki, Aoba-ku, Sendai, Miyagi 980-8578 (Japan)

[f] Dr. J. Šebera
Department of Functional Materials
Institute of Physics, Academy of Sciences of the Czech Republic, v.v.i.
Na Slovance 2, 182 21 Prague 8 (Czech Republic)

Supporting information for this article is available on the WWW under http://dx.doi.org/10.1002/chem.201300460.

Introduction

The metal linkage to nucleic acids (M–NAs) affects their properties significantly. These changes concern both the molecular structure and the function of M–NAs. It is well known that metals that naturally solvate NAs, such as Mg^II and others, govern their 3D folding and trigger/enhance many biochemical processes.[1] A rather special alternative of M–NAs concerns their modified base pairs in which usual hydrogen bonding is replaced by a metal-mediated interaction.[2] Even normal base pairs that occur naturally in DNA and RNA molecules are capable of such a metal linkage. As one can foresee, the physicochemical properties of metal-mediated and standard Watson–Crick base pairs may differ. The normal biochemical functions of NAs could be modified either in a desirable or destructive way. The latter effects have been reported particularly in the context of mercury uptake by living organisms because of its high toxicity.

The controllable preparation of M–NAs is considered promising regarding the usability of such materials in nanotechnology.[3] Understanding the bonding of metals to NAs is clearly essential for the targeted, rational design of novel materials based on M–NAs. Among other modifications, recently mentioned in connection with technological applications, the doping of NAs with heavy metals has been studied rather extensively. Promising proposals and functional materials include, for example, electric sensors, charge-transport

materials,[4–7] fluorescent and luminescent sensors,[8] and artificial NAs.[9]

The metal-mediated base pairs composed of natural NA bases possess one advantage. Natural NAs have been intensively studied over recent decades; therefore, methods for their preparation and characterization are well developed. The pyrimidine:pyrimidine mismatches, such as thymine:thymine (T:T) and cytosine:cytosine (C:C), are suitable for doping with metals. Spatial occupation of the pyrimidine-metal-pyrimidine base pairs within the DNA duplex resembles standard Watson–Crick purine–pyrimidine base pairs. However, other pseudo-base pairs linked with different metals have also been prepared by employing suitable organic compounds that substitute the role of natural bases.[10] For example, a silver linkage was studied in the C-Ag^I-C base pair.[11,12] The imidazole ring in the imidazole-Ag^I-imidazole pseudo-base pair appeared to be a functional alternative to normal cytosine.[13,14]

The T-Hg^{II}-T metal-mediated base pair is probably one of the best structurally resolved of these base pairs. The (T)N3-Hg^{II}-N3(T) metal-mediated linkage was unambiguously determined by means of the ^2J(N3,N3) NMR spin–spin J-coupling measured-across the linkage.[15] The heavy metal bonding to the imino nitrogen atom of thymine was characterized by using Raman spectroscopic analysis to be covalent with significant ionic character.[16,17] The B-form of Hg^{II}–DNA containing consecutive T-Hg^{II}-T base pairs was determined recently by means of NMR spectroscopic analysis.[18] Moreover, the reaction enthalpy and entropy values and the Gibbs free-energy of reaction for doping the mismatched T:T base pair with Hg^{II} ion are also known.[19]

Both the metal and the NA base are critical in establishing stable metal-mediated base pair with desired properties. Heavy-metal ions, such as Hg^{II}, differ in this respect from other lighter metal ions that typically solvate NAs. In particular, the closed-shell heavy-metal ions with a positive charge, for example Au^I, Ag^I, Tl^I, or Hg^{II}, attract each other owing to metallophilic attraction.[20] This metal–metal interaction, driven by dispersion forces and enhanced by relativistic effects, often remains stabilizing despite that the metal centers coordinated to organic molecules, such as NA bases, possess positive charge. The metallophilic attraction between mercury atoms in two consecutive T-Hg^{II}-T base pairs accounts roughly for 9% of the total stabilization.[21] Also the Ag^I–Ag^I interaction studied recently in M–NA base pairs was noticed.[22] The normal NA base pairs linked with metal ions, such as Hg^{II} and Ag^I, are apparently attractive with regard to their usability in nanotechnology because the heavy-metal ions may bring new unexpected properties to M–NAs.

Little is known about the chemical reactions for the formation of metal-mediated base pairs because the capture and characterization of individual states during these multistep processes is very difficult. The exact coordination of a metal center to nucleobases was determined only for few base pairs owing to lack of both the structures obtained from X-ray crystal studies and NMR spectroscopic analysis.

The stabilizing or destabilizing effect of a metal center, although measurable, is not sufficient for the full characterization of a base pair or to describe the chemical reactions. Thus, the character of a metal linkage remains usually unclear. As mentioned, the T-Hg^{II}-T base pair is probably the only exception in this regard. The T-Hg^{II}-T linkage was determined experimentally by using NMR and Raman spectroscopy, the structure of the base pair was resolved, and the thermodynamic parameters of the chemical reaction were measured.[15–18] These experimental data enabled us to propose and calculate the mechanistic pathway for the formation of the T-Hg^{II}-T DNA base pair in this study. Our aim was to obtain a reliable picture of the reaction that is coherent with available experiments.

Computational Details

Two types of structural model were employed in this study. The trinucleotide double-strand DNA (ds-DNA) model was used in the calculations of the stationary states (Figure 1). The ds-DNA molecule with G-C,T:T,T-Hg^{II}-T and G-C,T-Hg^{II}-T,T-Hg^{II}-T base pairs described the reactant and product, respectively. The calculations involved only the middle base pair of the ds-DNA molecule and the $[Hg^{II}(H_2O)_4OH]^+$ cluster. The other model, which consisted of N1-methylthymine molecule(s) (Figure 1b) and smaller Hg^{II}-aqua clusters was used in the calculations of the transition states. In addition, the $[Hg^{II}(H_2O)_nOH]^+$ ($n=1$–5) and $[Hg^{II}(H_2O)_n]^{2+}$ ($n=1$–6) clusters (i.e., the isolated Hg^{II}–aqua clusters) were also calculated.

The initial geometry of the ds-DNA reactant was derived from a B-DNA dodecamer containing the trinucleotide sequence of the reaction product that had been determined recently by using NMR spectroscopic experimental restrains.[18] The B-form of the ds-DNA model was preserved in all the calculations. To prepare a model of the reactant, the middle T-Hg^{II}-T base pair of the ds-DNA molecule was modified to the T:T base pair (Figure 1a). The $[Hg^{II}(H_2O)_4OH]^+$ cluster was coordinated to the T:T mismatch in the major groove of the ds-DNA molecule (Figure 1c,d).

The Morokuma two-layer ONIOM QM/QM method was used in the geometry optimizations of the stationary states.[23] Only the middle base pair of the ds-DNA molecule, including the sugars and $[Hg^{II}(H_2O)_4OH]^+$ cluster that defines the inner layer within the ONIOM model (Figure 1c,d), were geometry optimized. The rest of the ds-DNA molecule was kept fixed and the B-form of the trinucleotide was thus preserved in all the calculations. The inner layer was described with the B3LYP method.[24] The 6-31G(d) atomic basis was used.[25] The scalar energy-averaged Stuttgart effective core-potential (ECP) MWB-60 was employed for the Hg^{II} center in the inner ONIOM layer, whereas the outer layer was described with the BP86 method and LANL2DZ pseudopotential.[26] The B3LYP method, the 6-31+G(d) atomic basis, and the Stuttgart ECP for the Hg^{II} center were used in transition-state calculations that employed smaller structural models. The same method was also used for calculations of isolated Hg^{II} clusters. The implicit water solvent IEF-PCM/UFF (as default in Gaussian 09.A02) was used in all the calculations.[27]

The pK_a values for the hexa-aqua–Hg^{II} complexes were calculated by using the B3LYP method, 6-31++G(d,p) basis, and MWB-60 pseudopotentials for the mercury atom. The original basis set was augmented by one f-polarization function with exponent $\alpha_f=0.997$ and by a set of diffuse functions with exponents of $\alpha_s=0.0075$, $\alpha_p=0.0060$, and $\alpha_d=0.010$ in correspondence with the 6-31++G(d,p) basis sets. The same method was used for the geometry optimization of the Hg^{II}–aqua complexes. The pK_a values were also calculated with a larger set of 2f1g polarization functions of $\alpha_f=1.34$, 0.42, and $\alpha_g=1.33$. The polarization functions were
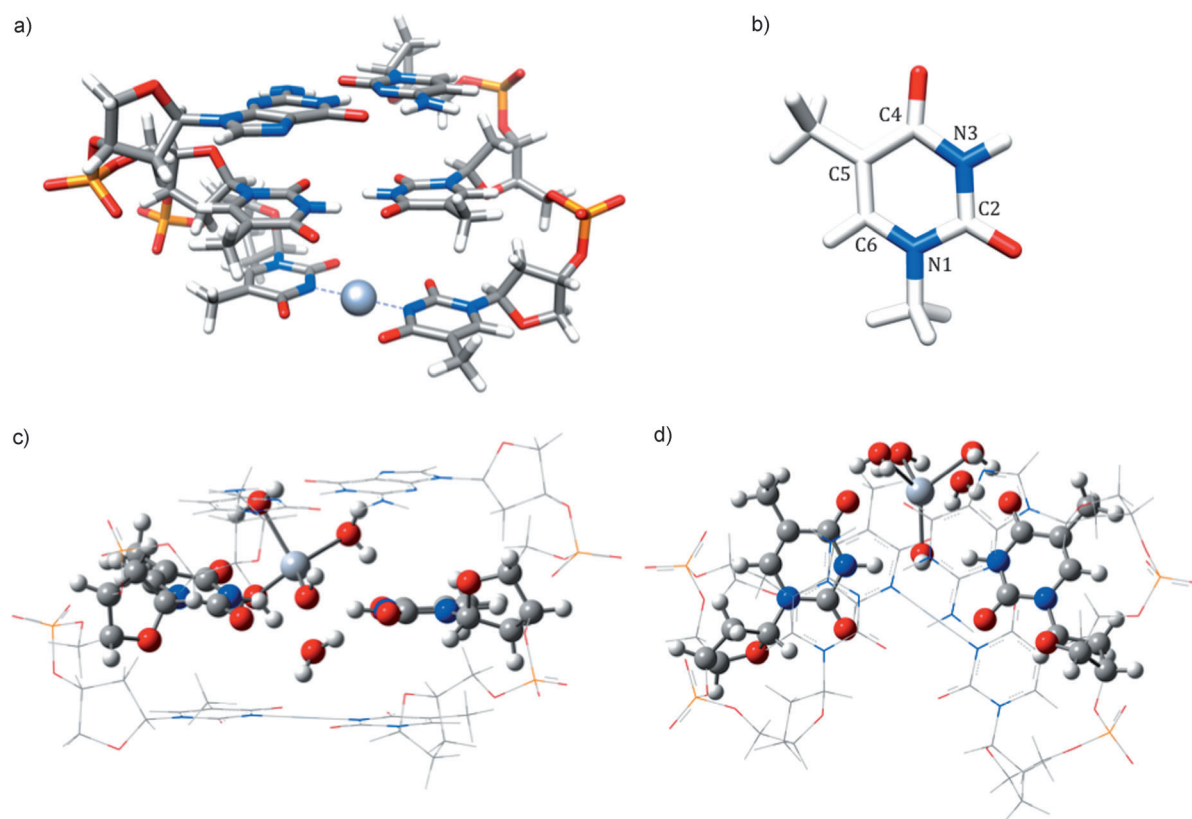
Figure 1. The structural models employed in this study. a) The ds-DNA molecule with middle T:T and terminal G:C and (T)N3-Hg^{II}-N3(T) base pairs. b) N1-methylthymine. c) The ds-DNA model of the reactant (the middle T:T base pair interacts with the [Hg^{II}(H$_2$O)$_4$OH]$^+$ cluster). d) The top view along the helical axis. The highlighted atoms in (c) and (d) defined the inner layer within the geometry-optimized ONIOM model.

optimized for a neutral Hg center in the ground state by using the coupled-cluster singles and doubles (CCSD) method.

The thermodynamic parameters were calculated for the stationary and transition states that were all checked with vibration-frequency analysis. The entropy ΔS and Gibbs free energy ($\Delta G = \Delta H - T\Delta S$) were calculated for temperature and pressure of 298.15 K and 101.325 kPa within the ideal-gas, rigid-rotor, and harmonic-oscillator approximation. The activation energies $\Delta G^{\pm}$ and $\Delta H^{\pm}$ were calculated as a difference of the respective energies for the transition state and reactant. The reaction energies ΔG_R and ΔH_R were calculated as difference of the respective energies for the product and reactant.

The FPMD simulations of the [Hg^{II}(H$_2$O)$_6$]$^{2+}$ and [Hg^{II}(H$_2$O)$_5$OH]$^+$ clusters were performed on the Born–Oppenheimer potential-energy surface calculated at the BP86/def2-SVP level.[28,29] The Leapfrog Verlet algorithm was used to update the coordinates. The threshold values for the energy and coupled perturbed Hartree–Fock (CPHF) equations convergence were tightened to 10^{-9} a.u to avoid numerical instabilities. The numerical grid denoted as "m5" was used, the time step was 10 a.u. (0.24188 fs), and the temperature was kept fixed at 300 K. The conductor-like screening model (COSMO) was used to simulate the solvent effect of the outer solvation shells.[30] Trajectories of nearly 1ps were finally evolved after the equilibration, which lasted 250 fs.

The Gaussian 09 (revision A02) program package was used to obtain the geometries and thermodynamic parameters.[31] The FPMD simulations were obtained by using the Turbomole 6.3.1 code.[32]

Results and Discussion

The Hg^{II} reactant: The reactant was described as a Hg^{II} ion surrounded by explicit molecules of solvent, that is, the Hg^{II}–aqua cluster. The outer overall hydration of the Hg^{II}–aqua cluster was obtained by using the implicit solvent model. Both the structure and the composition of the explicit solvent are key factors because the ligands of the Hg^{II} ion may act as a nucleophile. The nucleophilicity calculated for the OH$^-$ and H$_2$O ligands, which should be particularly considered for bulk water, appeared among others on the order HS$^-$ > OH$^-$ > Cl$^-$ > H$_2$O.[33] As can be foreseen, the hydroxo ligand is a much better nucleophile for proton abstraction than the aqua ligand, the possible occurrence of which at neutral pH has to be reflected by using a proper model considered for the mercury reactant.

The pK_a values of 5.6 and 5.8 for the hexa-aqua–Hg^{II} complex were calculated in this study by using the two approaches (see the Computational Details). The pK_a value of 3.6 measured in solution with water corresponded to one hydroxo ligand of the Hg^{II} ion at a neutral pH value.[34] The pK_a(II) values calculated by using the two approaches were pK_a 8.0 and 10.5. Calculations of the pK_a values generally require the use of highly accurate computational methods and

qualitatively correct descriptions of the solvent. Although the calculation methods used were reliable, both the sampling of molecular clusters that described the metal solvation and the description of the outer solvation shells were simplified. Despite the somewhat larger pK_a values calculated for the hexa-aqua–Hg^{II} complex, the calculations confirmed the occurrence of one hydroxo ligand of the Hg^{II} ion at a neutral pH value.

The Hg^{II}–hydroxo (one hydroxo ligand) and pure Hg^{II}–aqua clusters, including different number of explicit aqua ligands, were calculated to obtain their typical overall structure. Both the optimal geometry and the number of ligands that remained coordinated to the Hg^{II} center after geometry optimization in these two types of cluster differed systematically. In the [Hg^{II}(H$_2$O)$_n$OH]$^+$ ($n=1$–5) clusters, only the hydroxo ligand and the aqua ligand in the *trans* position to the OH$^-$ ion (the *trans*-aqua ligand) remained coordinated to the metal center (see Figure S1 in the Supporting Information). The remaining aqua ligands departed from the nearest hydration shell of the Hg^{II} center during the geometry optimization. These water molecules preferred water–water hydrogen-bonding interactions rather than coordination to the Hg^{II} ion. Note, the hydration of entire surface of the Hg^{II} center was ensured by aqua ligands or by implicit solvent (PCM) when these aqua ligands departed. The explicit solvation in Hg^{II}–hydroxo clusters consisted of the hydroxo and *trans*-aqua ligands only. Other aqua ligands/water molecules appeared freely exchangeable and their role seemed to be well substituted by the implicit solvent (PCM). In the [Hg^{II}(H$_2$O)$_n$]$^{2+}$ ($n=1$–6) clusters, only three aqua ligands were typically sustainable. The rest of the water molecules departed again from the nearest hydration shell of the Hg^{II} ion (see Figure S2 in the Supporting Information).

The distance of the hydroxo ligand from the Hg^{II} center in the calculated clusters was the shortest of all the other ligands, that is, $r_{\text{Hg–O(OH)}} = 2.09$–2.14 Å. Even slightly shorter $r_{\text{Hg–O(OH)}}$ distances were calculated in the Hg^{II}–aqua clusters by using the same DFT functional and different basis set and with the MP2 method.[33,35] Though virtually similar, the slightly longer $r_{\text{Hg–O(OH)}}$ distance seemed to be due to the implicit water solvent employed on top of the explicit one in our calculations. The *trans*-aqua ligand in the Hg^{II}–hydroxo clusters was longer, that is, $r_{\text{Hg–O(H2O)}} = 2.28$–2.56 Å. The two ligands and the Hg^{II} center aligned linearly. The linear arrangement of the *trans*-aqua ligand with the thymine anion was important for the studied reaction (see below). The overall distances of three typical aqua ligands from the Hg^{II} center in pure Hg^{II}–aqua clusters were the longest of all the ligands, that is, $r_{\text{Hg–O(H2O)}} = 2.41$–2.61 Å. The three aqua li-

gands appeared to be structurally equivalent; namely, the O-Hg-O bonding angles were close to 120°, and the ligands were in one plane with the Hg^{II} center.

The FPMD simulations of the [Hg^{II}(H$_2$O)$_5$OH]$^+$ and [Hg^{II}(H$_2$O)$_6$]$^{2+}$ clusters in Figure 2 confirmed the static picture obtained from the optimized geometries. The initial ar-
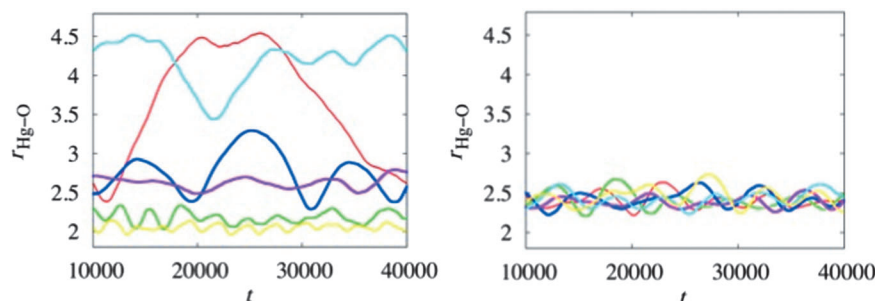

Figure 2. The distances of the solvent molecules from the Hg center obtained during the first-principles molecular dynamics (FPMD) simulation for the [Hg^{II}(H$_2$O)$_5$OH]$^+$ (left) and [Hg^{II}(H$_2$O)$_6$]$^{2+}$ (right) complexes. The $r_{\text{Hg–O}}$ distances are given in Å and time is in a.u. (1 a.u. = 0.024188 fs). The distances for the hydroxo and *trans*-aqua ligand in the [Hg^{II}(H$_2$O)$_5$OH]$^+$ simulation are marked in yellow and green, respectively.

rangement of the solvent molecules that surrounded Hg^{II} ion was octahedral, and the initial distances of the ligands corresponded to those in the optimized geometries. In the [Hg^{II}(H$_2$O)$_5$OH]$^+$ simulation, only the hydroxo and the *trans*-aqua ligand remained coordinated to the Hg^{II} center, other water molecules had moved away. The distances of two distinguished ligands from the Hg center did not exceed 2.3 Å, and the hydroxo ligand was always closer to the Hg center. The distances of the water molecules fluctuated between 2.5 and 4.5 Å, thus indicating their loose coordination to the Hg center. In fact, two of them had clearly moved from the inner coordination shell of the Hg^{II} center. The water molecules in the hexa-aqua complex were equivalent during the simulation, and their distances from the Hg center fluctuated between 2.2 and 2.7 Å.

In short, the DFT and FPMD results indicated coherently the overall hydration pattern of the Hg^{II} center; that is, the hydroxo and *trans*-aqua ligand in the Hg^{II}–hydroxo clusters are more strongly bound relative to the three loosely bound aqua ligands in pure Hg^{II}–aqua clusters. Other water molecules in proximity to the Hg^{II} center appeared freely exchangeable. The Hg^{II}–hydroxo type of cluster occurs at a neutral pH value. The [Hg^{II}(H$_2$O)$_4$OH]$^+$ cluster was employed as a Hg^{II} reactant in this study.

Sketch of the reaction pathway: The mechanistic pathway for the formation of the T-Hg^{II}-T metal-mediated base pair proposed in this study included, among others, the following key steps: The formation of the first (T)N3–Hg^{II} bond was described with two steps. The abstraction of the imino proton from thymine by the hydroxo ligand allowed the substitution of the imino proton with the Hg^{II} ion. The imino proton and hydroxo ligand formed a water molecule. The interaction of thymine with the [Hg^{II}(H$_2$O)$_4$OH]$^+$ cluster can be described as given in Equation (1).

$$[(T)N3-H] + [Hg^{II}(H_2O)_4OH]^+$$
$$\rightarrow [(T)N3-Hg^{II}(H_2O)_4]^+ + H_2O \tag{1}$$
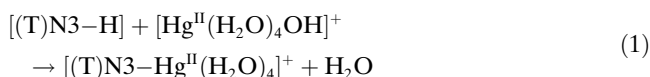
The second linkage of the Hg^{II} center with the remaining thymine base was conditioned through thymine tautomerization and also resulted in the release of the imino proton. The imino proton and water molecule coordinated to the DNA strand gave rise to the oxonium ion, whereas the neutral T-Hg^{II}-T base pair was formed. The Hg^{II} center was completely dehydrated during this reaction step [Eq. (2)].

$$[(T)N3-Hg^{II}(H_2O)_4]^+ + [H-N3(T)]$$
$$\rightarrow [T(N3)\text{-}Hg^{II}\text{-}(N3)T] + (H_2O)_4 + H_3O^+ \tag{2}$$
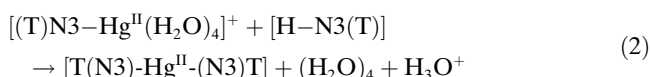
The two (T)N−Hg^{II} bonds in the metal-mediated base pair were chemically equivalent. However, their nonequivalent formation was proposed to explain the initial solvation of the Hg^{II} ion with one hydroxo ligand at a neutral pH value. According to the proposal, one linkage is formed by an attack of the hydroxo ligand on the base imino hydrogen atom, whereas the other linkage is triggered through tautomerization of the metal-nonbonded thymine base. As can be foreseen, the abstraction of the imino proton could be in principle facilitated by protonation of the nucleobases in both the cases. The effect was actually calculated, but only for the abstraction of the imino proton brought about by the hydroxo ligand.

Geometries of the stationary states along the reaction pathway: The stationary states were calculated by employing the ds-DNA molecule and [Hg^{II}(H$_2$O)$_4$OH]$^+$ reactants. The geometry parameters calculated for the stationary states can be found in Table S1 (see the Supporting Information). The interaction of the Hg^{II}–hydroxo cluster with the T:T mismatched base pair occurred in the major groove of the ds-DNA molecule. In reactant R, the hydroxo ligand coordinated to the imino hydrogen atom of thymine to fulfil the prerequisite that assumes its abstraction with the nucleophile. The interaction of the Hg^{II} center with the ds-DNA molecule was mediated by the aqua ligands, except for one close contact to the carbonyl O4 atom exposed to the major groove ($r_{(T)O4-Hg} = 2.660$ Å). The tight coordination of the hydroxo ligand to the imino hydrogen atoms represented the state just before proton abstraction ($r_{(OH)O-H3(T)} = 1.711$ and 1.760 Å). The distances of the aqua ligands from the Hg^{II} center in the R state were similar to the distances in the isolated clusters ($r_{(OH)O-Hg} = 2.243$ and $r_{(H_2O)O-Hg} = 2.474$–2.509 Å). Only one aqua ligand moved away during the geometry optimization and coordinated to the carbonyl group of one thymine base ($r_{(H_2O)O-Hg} = 3.486$ Å). The initial distances of the Hg^{II} center from the imino nitrogen atoms in the R state were 3.749 and 3.785 Å.

Prior to the first Hg^{II}–N3(T) linkage in the IS1 state, the imino proton was abstracted by the hydroxo ligand. The respective activation barrier was calculated (see below). The water molecule formed in IS1, owing to the association of

the imino proton and hydroxo ligand, coordinated to both the DNA strand and the Hg^{II} center ($r_{(H_2O)H-O2(T)} = 1.651$, and $r_{(H_2O)O-H3(T)} = 1.729$, and $r_{(H_2O)O-Hg} = 2.971$ Å). The proton abstraction disclosed the imino nitrogen atom for Hg^{II} coordination ($r_{(T)N3-Hg} = 2.387$ Å), although the Hg center was coordinated also to the neighbouring carbonyl group ($r_{(T)O4-Hg} = 2.626$ Å). The initial coordination of the Hg center to the base carbonyl group in R ($r_{(T)O4-Hg} = 2.660$ Å) was lost in the IS1 state ($r_{(T)O4-Hg} = 3.478$ Å). The disclosed imino nitrogen atom appeared to be a more favorable site for the coordination of the Hg^{II} center than the base carbonyl group.

The second Hg^{II}–N3(T) linkage was also conditioned by a disclosure of the respective imino site. As an alternative, we proposed the water-mediated tautomerization of the metal-nonbonded thymine base. The respective activation barrier was also calculated (see below). In the IS2 state, the imino proton transferred to the carbonyl O2 atom owing to tautomerization, but the imino nitrogen atom was still hindered by a water molecule ($r_{(H_2O)H-N3(T)} = 1.938$ Å). The coordination of the Hg center to the neighbouring carbonyl O4 atom that had occurred in IS1 was lost in the IS2 state ($r_{(T)O4-Hg} = 2.857$ Å). The Hg^{II}–N3(T) linkage already established in the IS1 state was further stabilized ($r_{(T)N3-Hg} = 2.267$ Å).

The interaction of the Hg^{II} ion with the thymine tautomer in the IS2 state was mediated with two water molecules ($r_{(H_2O)O-Hg} = 2.419$ and 2.485 Å). The release of one of these bridging water molecules in the IS3 state ($r_{(H_2O)O-Hg} = 2.238$ and 3.500 Å) was accompanied by shortening of the Hg^{II}–N3(T) bond ($r_{Hg-N3(T)} = 2.180$ Å). Both the aqua ligands and Hg^{II} center bridged the base pair in the IS2 and IS3 states. The N3-Hg-O(H$_2$O) bond angle in the IS3 state was 160°. We may assume that the linear arrangement of the *trans*-aqua ligand to the thymine anion in the IS3 state was stabilized in a similar manner to the *trans*-aqua ligand in isolated Hg^{II}–hydroxo clusters. The strong *trans* effect has been already reported for other anionic ligands of the Hg^{II} ion.[33] In our case, the *trans* effect contributed to the stability of the pseudo-base pair and prevented its opening. The other water molecules, which were only loosely coordinated to the Hg^{II} center, may be released to bulk relatively easily.

The (T)N3-Hg^{II}-O4(T) metal-mediated linkage was calculated only in the IS4 state, the first intermediate stabilized energetically (see below; $r_{(T)N3-Hg} = 2.192$, $r_{(Ttauto)O4-Hg} = 2.235$, $r_{(Ttauto)N3-Hg} = 2.917$ Å; Ttauto = thymine tautomer; N3-Hg^{II}-O4 = 176°). The explicit hydration of the Hg^{II} center was removed and all the water molecules coordinated on the ds-DNA molecule surface ($r_{(H_2O)O-Hg} = 3.657$–4.355 Å); thus, the IS5 state described the (T)N3-Hg^{II}-N3(T) linkage, which had been validated experimentally.[36] However, the bonding of the Hg^{II} center with the thymine tautomer was still shared by the N3 and O4 atoms ($r_{(Tauto)N3-Hg} = 2.258$, $r_{(Tauto)O4-Hg} = 2.694$ Å). The two $r_{(Tauto)O4-Hg}$ distances across the proper linkage involving the thymine anion in product P ($r_{(T)N3-Hg} = 2.172$ Å) were little longer ($r_{(Tauto)O4-Hg} = 3.030$ and 2.875 Å).

The N3-Hg-N3 bond angle in IS5 was 169°. The linear N3-Hg^{II}-N3 bond was calculated only for product P when the proton of the thymine tautomer was abstracted by water

within the minor groove in the ds-DNA molecule. The respective activation energy was calculated (see below). The P state was described by the neutral T-Hg^{II}-T base pair, four water molecules coordinated within the major grove and one H$_3$O$^+$ ion within the minor groove in the ds-DNA molecule. In the deprotonated P−H$^+$ state, the two Hg^{II}−N3(T) bonds were equivalent ($r_{(T)N3-Hg} = 2.154$ Å). The P−H$^+$ state represented the proper neutral reaction product that had been characterized experimentally.[36]

Activation energies along the pathway: The transition states calculated in this study were associated with three important reaction steps. TS1 described the substitution of the imino proton in thymine by the Hg^{II} ion, which was operated by the hydroxo ligand. TS2 described the water-assisted tautomerization of thymine (H3→O2). TS3 described the deprotonation of the carbonyl O2 atom in the T-Hg^{II}-T base pair ((O2)H$^+$→H$_2$O). The stationary states associated with these individual transition states were called reactants and intermediates. To avoid any possible confusion, the intermediates associated with transition states TS1–TS3 are marked by an apostrophe (see Figures 4–6 and Figures S3 and S4 in the Supporting Information). The initial geometries of the transition-state calculations were derived from the optimized geometries of the stationary states with the ds-DNA model.

The substitution of the imino hydrogen atom in thymine by the Hg^{II} center was calculated with the model that consists of the N1-methylthymine and [Hg^{II}(H$_2$O)OH]$^+$ reactants (Figure 4). The hydroxo ligand coordinated to the imino hydrogen atom and the *trans*-aqua ligand coordinated to the carbonyl O2 atom ($r_{(T)H3\cdots O(OH-)}$ = 1.713 and $r_{(T)O2\cdots H(H_2O)}$ = 1.789 Å). The geometry was similar to that of the R state with the ds-DNA model in Figure 3. The activation and reaction energies calculated for the abstraction of the imino proton were $\Delta G^\ddagger = 2.9$ and $\Delta G_R = 1.6$ kcal mol^{-1}, respectively. The reaction energy for the substitution of the imino hydrogen atom by the Hg^{II} center was $\Delta G_R = -1.3$ kcal mol^{-1}. The IS1′ state with a higher ΔG_R value described the situation in which the imino site was hindered by water, whereas the IS2′ state described full co-

ordination of the Hg^{II} center ($r_{Hg-N3(T)} = 4.087$ and 2.317 Å for IS1′ and IS2′, respectively). The values $\Delta G^\ddagger = 1.0$ and $\Delta G_R = -0.2$ kcal mol^{-1} were calculated for the abstraction of the imino proton by a free hydroxide ion (see Figure S3 in the Supporting Information). The calculation indicated the most likely exchange process for this alternative reaction, which may nevertheless facilitate coordination of the Hg^{II} center to thymine.

For the linkage of the metal-bonded base (T)N3−Hg^{II} with the metal-nonbonded thymine base, we assumed that water-assisted tautomerization occurred. The imino proton of the metal-nonbonded thymine transferred to the carbonyl O2 atom owing to the tautomerization. The water-assisted tautomerization for the thymine ion had already been proposed and calculated.[37] A recent study for neutral thymine unveiled a decrease in the activation barrier for proton transfer owing to microsolvation with different metals.[38] In our case, the water molecule that mediated proton transfer was coordinated both to the imino hydrogen atom and to the carbonyl O2 atom (Figure 5). The occurrence of a water molecule within the base pair that lacks a direct interbase linkage might be assumed. The bridging water molecule
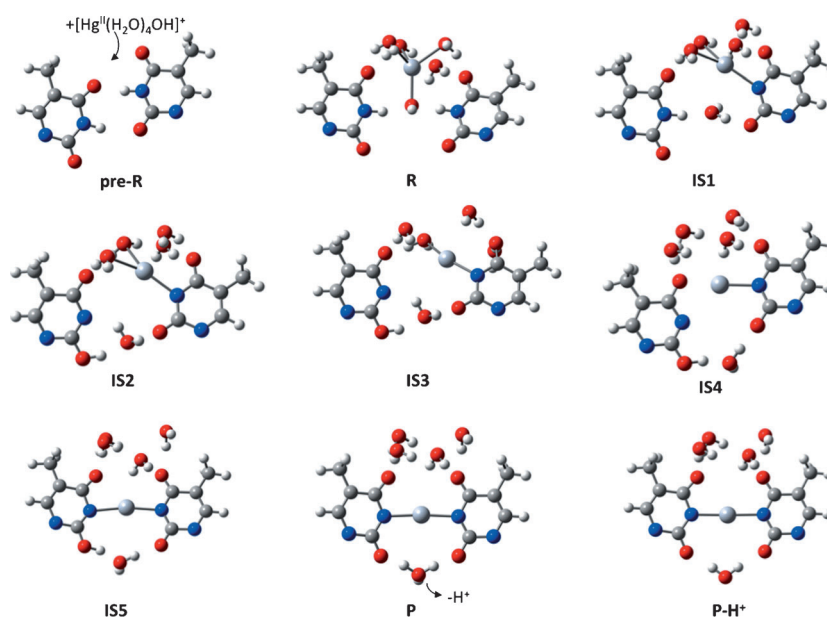

Figure 3. The geometries of the middle base pair in the ds-DNA molecule that interacted with the [Hg^{II}-(H$_2$O)$_4$OH]$^+$ cluster calculated for the stationary states along the reaction pathway: pre-R = pre-reactant (mismatched T:T base pair), R = reactant, IS1–IS5 = intermediate states, P = product (including H$_3$O$^+$), and P−H$^+$ = product (deprotonated H$_3$O$^+$). Note that the complexes in the R, IS1-IS5, and P states have a charge of +1.
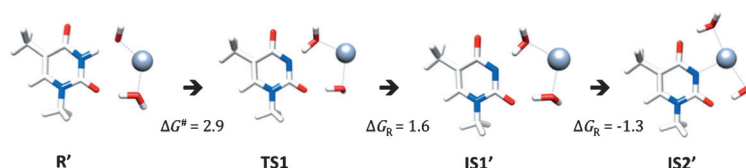

Figure 4. The Gibbs free energies in kcal mol^{-1} referenced to the energies for reactant R′ calculated for the substitution of the imino hydrogen atom in thymine by the Hg^{II} ion.
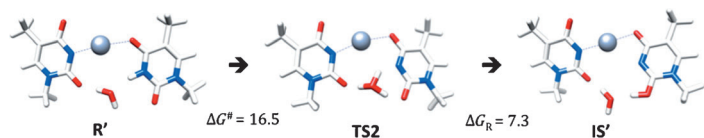
Figure 5. The Gibbs free energies in kcal mol^{-1} referenced to the energies for reactant R′ calculated for the water-assisted tautomerization of the thymine base.

Figure 6. The Gibbs free energies in kcal mol^{-1} referenced to the energies for reactant R′ calculated for the deprotonation of the T-Hg^{II}-T base pair.

may also appear owing to the association of the imino proton and hydroxo ligand according to our reaction scenario. In the R′ state, the water oxygen atom that mediated the tautomerization was coordinated to the imino hydrogen atom of the thymine base ($r_{(T)H3\cdots O(H_2O)}=1.786$ Å), whereas the hydrogen atom was further from the carbonyl O2 atom ($r_{(T)O2\cdots H(H_2O)}=2.837$ Å). The H_3O^+ species was formed in the transition state ($r_{(T)H3\cdots O(H_3O+)}=1.009$, $r_{(T)N3\cdots H3(H_3O+)}=1.820$, and $r_{(T)O2\cdots H(H_3O+)}=1.420$ Å). The imino site was disclosed for the coordination of the Hg^{II} ion after tautomerization in the IS′ state. The coordination of the bridging water molecule to the thymine anion remained similar during the three steps ($r_{(T)O2\cdots O(H_2O)}=2.735$, 2.735, and 2.730 Å), whereas the coordination to the thymine tautomer changed ($r_{(T)O2\cdots O(H_2O)}=3.265$, 2.464, and 2.616 Å). The $r_{(T)N3\cdots O4(T)}$ distance across the N3-Hg^{II}-O4 linkage decreased from 4.478 to 4.457 and 4.422 Å for the R′, TS2, and IS′ states, respectively. The geometry of the base pair in IS′ was similar to the geometry for the IS4 state (Figure 3). The activation and reaction energies for the tautomerization were $\Delta G^{\neq}=16.5$ and $\Delta G_R=7.3$ kcal mol^{-1}, respectively.

As an alternative to the water-assisted tautomerization, we also considered thymine deprotonation by the hydroxo ligand of the Hg^{II} ion already coordinated to the thymine base (see Figure S4 in the Supporting Information). This alternative reaction may occur, assuming either the di-hydroxo–Hg^{II} cluster as an initial Hg^{II} reactant or upon coordination of a free OH$^-$ ion to the Hg^{II} ion already coordinated to thymine, which could be both possibly obtained upon variation of the pH value. The alternative pathway possessed a lower activation energy and a higher reaction energy ($\Delta G^{\neq}=13.5$ and $\Delta G_R=9.9$ kcal mol^{-1}, respectively) relative to the water-assisted tautomerization. Therefore, neither the tautomerization nor the alternative mechanism seemed to be the preferential pathway, which is in agreement with sustainable stability of the T-Hg-T base pair measured upon variation of the pH value.[36]

The base pair with the proper N3-Hg^{II}-N3 linkage calculated for the IS5 state in Figure 3 was still protonated owing to tautomerization. We assumed that the proton at the carbonyl O2 atom is absorbed by bulk water because the neutral base pair was observed. The base-pair deprotonation employed the bridging water molecule that mediated the tautomerization (Figure 6). The (T)N3−Hg distances in the R′ and IS′ states were $r_{(T)N3-Hg}=2.205$, 2.257 and 2.205, 2.198 Å, respectively. The activation and reaction energies for deprotonation were $\Delta G^{\neq}=0.1$ and $\Delta G_R=0.5$ kcal mol^{-1}, respectively.
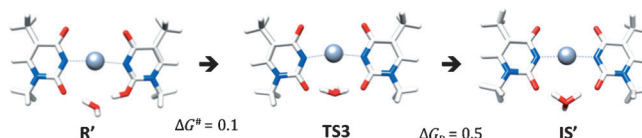
Free-energy profile of the reaction pathway: The unified picture of the formation of the T-Hg^{II}-T base pair was obtained by using the calculated reaction and activation energies. The ds-DNA model ensured the correct molecular environment of the base pair where the reaction occurred. The stepwise penetration of the Hg^{II} ion into the central part of the double helix was described properly; in particular, the dehydration of the Hg^{II} ion during the reaction that had been validated experimentally[18] was achieved with the ds-DNA model. The activation energies calculated with smaller models complemented the free-energy landscape (Figure 7). Although the local geometries calculated with smaller and ds-DNA models for virtually corresponding intermediates did not match exactly, they were chemically equivalent. The inclusion of $\Delta G^{\neq}$ energies into the free-energy reaction profile was therefore possible, and the unified free-energy landscape that described whole reaction was obtained.

The first Hg^{II}−N3(T) linkage was triggered by abstraction of the imino proton by the hydroxo ligand of Hg^{II} ($G^{\neq}=2.9$ kcal mol^{-1} for TS1). The reaction energy for the substitution of the imino proton by the Hg^{II} ion calculated, by using the small model in Figure 4, was $\Delta G_R=-1.3$ kcal mol^{-1}. The reaction energy for the structurally equivalent IS1 state in Figure 3 was $\Delta G_R=1.4$ kcal mol^{-1}. The second (T)N3−Hg^{II} linkage proceeded after the water-assisted tautomerization of the metal-nonbonded thymine (Figure 5), alternatively through thymine deprotonation with the hydroxo ligand of the Hg^{II} ion already coordinated to thymine (see Figure S4 in the Supporting Information). The activation energy for tautomerization was $\Delta G^{\neq}=16.5$ kcal mol^{-1}, and the activation energy calculated for the tautomerization of isolated thymine mediated with one water molecule was $\Delta G^{\neq}=22.4$ kcal mol^{-1}.[38] The relatively lower activation barrier obtained in this study was due to coordination of the Hg^{II} ion to the carbonyl O4 atom (Figure 5). The polarization of the carbonyl O4 atom by the ion enhanced the abstraction of the imino proton. Even better enhancement was calculated owing to protonation of the O4 atom. The reactant-like complex similar to the R′ state in Figure 4 but with a protonated carbonyl O4 atom was not stable because the proton abstraction by the hydroxo ligand was spontaneous upon the thymine protonation (data not shown). Therefore, we assumed that nucleobase protonation would scale down the activation barriers for the abstraction of the imino proton and the tautomerization.

The reaction energy calculated for the base-pair tautomerization in Figure 5 was $\Delta G_R=7.3$ kcal mol^{-1}. The reaction energy for the IS2 state, including the thymine tautomer in
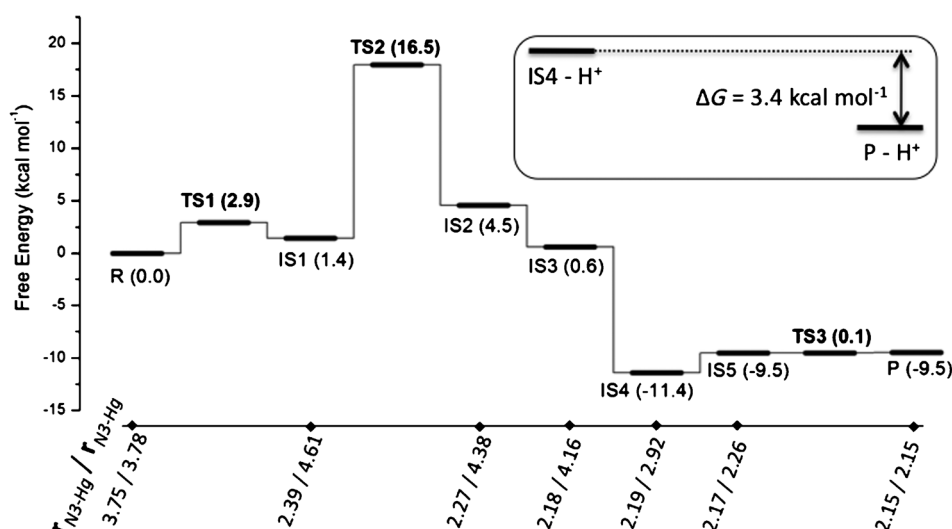
Figure 7. The Gibbs free energies ΔG_R calculated for intermediate states IS1–IS5 and product P, and the activation Gibbs free energies $\Delta G^{\neq}$ calculated for the TS1–TS3 states. The reaction energies ΔG_R referenced to the energy for reactant R were calculated with the ds-DNA model in Figure 1. The geometries for the stationary states are depicted in Figure 3 The $\Delta G^{\neq}$ energies for the TS1–TS3 states were calculated by using the structural models depicted in Figures 4–6, respectively. The distances of the Hg^{II} center from the imino nitrogen atoms of the thymine bases are given below the graph in Å. Note that the overstabilization of the IS4 state was obtained owing to the protonated T-Hg^{II}-T base pair, whereas the Gibbs free energy for P–H$^+$ (deprotonated product) was below the energy for the IS4–H$^+$ state (see the small graph in the right corner and the explanation in the text). The chemical diagram of the reaction pathway is shown in Figure 8.

Figure 3, was $\Delta G_R = 4.5$ kcal mol^{-1}. In fact, the local bonding in the base pair for the TS2 state corresponded better to the IS4 state when the Hg^{II} center was completely dehydrated. The isolated pseudo-base pair, including bridging water molecules, in IS2 was not sustainable in base-pair-like topology when it was geometry optimized. The activation energy for the thymine tautomerization within the energy profile was therefore approximated with the energy for the TS2 state, which was placed between the energies for the IS1 and IS2 states in Figure 7.

When the first Hg^{II}–N3(T) linkage occurred, hydration of the Hg^{II} center was partially removed owing to competitive hydrogen bonding of the aqua ligands to the carbonyl groups. Only the *trans*-aqua ligand that mediated the linkage of two thymine bases was sustainable until the IS3 state, with $\Delta G_R = 0.6$ kcal mol^{-1}.

The first negative ΔG_R value along the pathway was calculated for the IS4 state. The Hg^{II} ion already linked to the thymine anion was also coordinated to the carbonyl O4 atom of the thymine tautomer ($\Delta G_R = -11.4$ kcal mol^{-1}). The N3-Hg^{II}-O4 metal-mediated linkage and dehydration of the Hg^{II} ion were characteristic features of the first stable intermediate. Note that the base pair in the IS4 state was still protonated owing to tautomerization.

The bonding of the Hg^{II} ion to the thymine tautomer in the IS5 state was shared by the O4 and N3 atoms. The Hg^{II} ion got closer to the protonated carbonyl O2 atom in IS5 when we considered the geometry of the preceding state, which may explain the poorer stabilization of the IS5 state ($\Delta G_R = -9.5$ kcal mol^{-1}).

The linear N3-Hg^{II}-N3 bond was calculated only for the reaction product P with a deprotonated carbonyl O2 atom ($\Delta G_R = -9.5$ kcal mol^{-1}). The H$_3$O$^+$ species were coordinated to the carbonyl O2 atoms in the T-Hg^{II}-T base pair, which was formally neutral. The activation energy for the deprotonation was $\Delta G^{\neq} = 0.1$ kcal mol^{-1}. The neutral P–H$^+$ state with a neutral solvent surrounding the T-Hg^{II}-T base pair was also geometry optimized.

The IS4 state was the most stable among all the stationary states calculated. The extraordinary stability of IS4 was puzzling because the occurrence of the N3-Hg^{II}-O4 linkage would be in conflict with the experiment.[36,16] As already mentioned, the base pair in IS4 was protonated, whereas the experimentally observed base pair was neutral. Therefore, the deprotonated IS4 state was also geometry optimized and its energy was compared with the energy for product P–H$^+$. The Gibbs free energy for P–H$^+$ was below the energy for the IS4–H$^+$ state by $\delta\Delta G_R = 3.4$ kcal mol^{-1} (Figure 7). To exclude the possible effect of the different explicit hydration in the two states on the calculated energies, all the water molecules were removed and hydration was modeled only with the implicit polarizable continuum model (PCM). The Gibbs energy for the deprotonated product P–H$^+$ was again lower, now by $\delta\Delta G_R = 9.1$ kcal mol^{-1}. The overstabilization of the N3-Hg^{II}-O4 linkage is therefore possible, but only in the protonated base pair.

The reaction enthalpy ΔH and entropy ΔS referenced to the thermodynamic parameters for reactant R were calculated for the IS1–IS5 states and for product P (see Table S2 in the Supporting Information). The values of $\Delta H = 0.4$, 4.6, 2.6, -8.1, -4.9, and -4.7 kcal mol^{-1} were obtained for the states. The first negative enthalpy along pathway was calculated again for the IS4 intermediate ($\Delta H = -8.1$ kcal mol^{-1}). The entropy of reaction $\Delta S = -3.4$ cal mol^{-1} K^{-1} was calculated for the IS1 state; however, all the consecutive ΔS values appeared above zero and increased monotonously up to $\Delta S = 16.0$ cal mol^{-1} K^{-1} for product P. The reaction enthalpy and entropy of reaction calculated for product P with respect to reactant R were $\Delta H_R = -4.7$ kcal mol^{-1} and $\Delta S_R = 16.0$ cal mol^{-1} K^{-1}, respectively. The calculated thermodynamic parameters agreed with the experiment by Torigoe et al. (Table 1).[19,39]

The positive value of the reaction entropy measured for the formation of the T-Hg^{II}-T base pair could be explained

Table 1. Comparison of the reaction enthalpy ΔH_R, Gibbs free reaction energy ΔG_R, and reaction entropy ΔS_R calculated in this study[a] with experiment.

Method	ΔH_R [kcal mol^{-1} K^{-1}]	ΔG_R [kcal mol^{-1} K^{-1}]	ΔS_R [cal mol^{-1} K^{-1}]
B3LYP	−4.7	−9.5	16.0
exp.[b]	−4.76 ± 0.13	−7.91 ± 0.12	10.6 ± 0.84
exp.[b]	−3.85 ± 0.18	−7.76 ± 0.19	13.1 ± 0.65

[a] The thermodynamic parameters were calculated for product P sketched in Figure 3 by using the ONIOM (B3LYP:BP86) method and referenced to the parameters for reactant R. [b] Experiment by Torigoe et al.[19]

by dehydration of the Hg^{II} center during the reaction provided that the hydration state of both the reactant and product is known. Only recently, we proved that the structurally ordered hydration shell of the Hg^{II} ion assumed in bulk is removed completely upon the formation of the metal-mediated base pair and the structurally disordered water molecules (former aqua ligands) are released to bulk.[18] Such a chemical process is virtually coherent with an increase in the reaction entropy. In any case, the chemical bonding that changed during the reaction affects also entropy, and the effect was calculated in this study.

The hydrogen bonding in the T:T mismatched base pair was changed to the N3-Hg^{II}-N3 metal-mediated bonding. According to our reaction proposal, several chemical changes occurred. The two imino protons were removed and released to bulk during the reaction. One proton was associated with the hydroxo ligand of the Hg^{II} ion, and the other proton was released to bulk, thus forming an oxonium ion. Thus, the dehydration of the Hg^{II} center occurred alone, with rather dramatic changes in the chemical bonding of the interbase linkage and the local bonding within the thymine nucleobase. The calculations deepened our understanding of the effect of the changed chemical bonding on the peculiar positive reaction entropy. The increase in the ΔS_R value along the pathway was obtained owing to the vibration entropy contributions (data not shown). The N3−Hg^{II} bond was previously characterized as covalent–ionic with a bond order smaller than that of the normal N3−H3 bond in thymine. The vibrations of the carbonyl groups shifted toward lower frequency upon the Hg^{II} uptake.[16] The number of vibrations calculated in thymine shifted down owing to the Hg^{II}-mediated linkage of the thymine bases (data not shown). We therefore assume that the entropy increase measured during the formation of the T-Hg^{II}-T base pair occurred owing to both the dehydration of the metal ion and the downshift of the number of the vibration frequencies.

The rate-limiting step of the reaction was the formation of the second linkage of the Hg^{II} ion to the metal-nonbonded thymine. Two mechanisms were proposed and modeled for this reaction step; that is, a water-assisted imino proton transfer to the carbonyl O2 atom of thymine and a substitution of the imino hydrogen atom in the mercury-nonbonded thymine base by a OH$^-$ ligand of the Hg^{II} center. The tautomerization and the alternative reaction possessed activation energies of $\Delta G^{\neq} = 16.5$ and 13.5 kcal mol^{-1}, respectively. The activation energy for the abstraction of the imino proton triggered by the hydroxo ligand of the hydrated Hg^{II} ion followed by the first Hg–thymine linkage was only $\Delta G^{\neq} = 2.9$ kcal mol^{-1}. The protonation of carbonyl group of thymine should provide even lower activation energies for both the thymine tautomerization and the abstraction of the imino proton.

The calculated reaction enthalpy was $\Delta H = -4.7$ kcal mol^{-1}, the reaction Gibbs free energy was $\Delta G_R = -9.5$ kcal mol^{-1}, and the reaction entropy was $\Delta S = 16.0$ cal mol^{-1} K^{-1}. The calculated thermodynamic parameters agreed with the experimental data by Torigoe et al.[19,39] The positive value of the reaction entropy was explained as an effect of both dehydration of the metal ion and a change in the chemical bonding during the reaction.

We have proposed the following reaction scenario based on agreement of the calculated and experimental data (Figure 8). The formation of the first Hg^{II}−N3(T) bond, facilitated by the hydroxo ligand of the Hg^{II} ion, proceeds with a relatively small activation barrier. The hydroxo ligand assumed at a normal pH value is essential for the low activation barrier of the first Hg–thymine linkage. The second linkage appears to be conditioned either by the tautomerization of the remaining Hg^{II}-nonbonded thymine base or by deprotonation by the hydroxo ligand of the Hg^{II} ion already bound to the thymine base. The second Hg–thymine linkage is energetically more demanding and represents the rate-limiting step of reaction. The *trans*-aqua ligand of the Hg^{II} ion already bound to the thymine anion contributes to the stability of the water-mediated base pair before the regular linkage occurs. In the protonated T-Hg^{II}-T base pair, the N3-Hg^{II}-O4 linkage is more stable than the regular N3-Hg^{II}-N3 linkage. Therefore, we hypothesize that the overstabilization of the irregular linkage for the protonated base pair might be the driving force of the reaction because the intermediate following rate-limiting step might be captured efficiently in this way. When the second imino proton is released to bulk the regular N3-Hg^{II}-N3 linkage is stabilized dominantly in full correspondence with the experimental data.

Conclusion

The reaction mechanism for the formation of the T-Hg^{II}-T metal-mediated base pair has been proposed and calculated. The chemical reaction basically involved substitution of imino protons in the T:T mismatched base pair with a Hg^{II} ion.

Acknowledgements
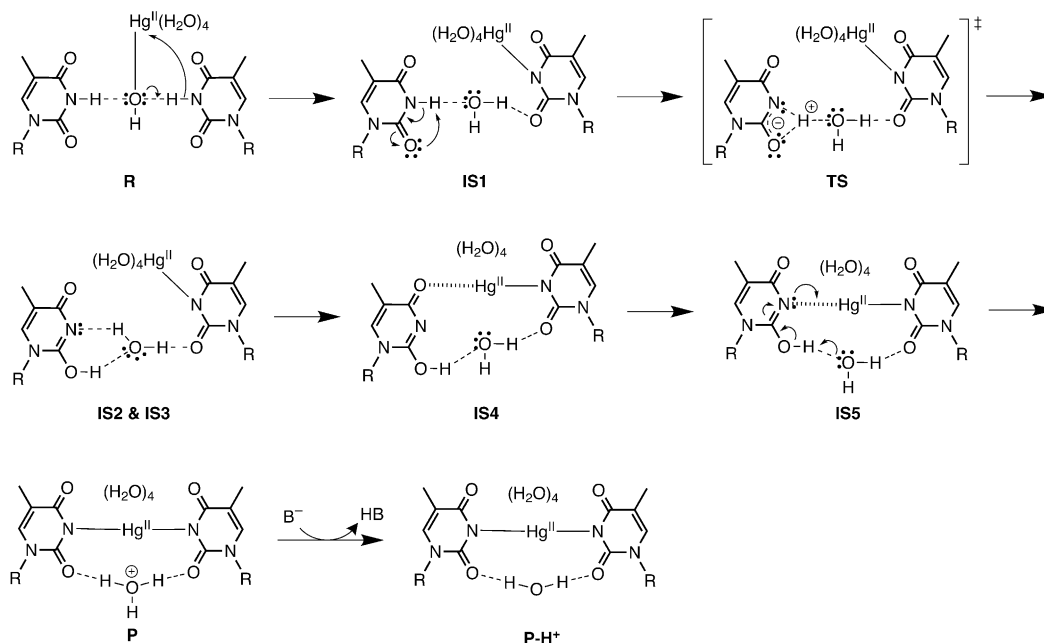
Figure 8. The chemical diagram of the calculated reaction pathway.

[1] A. Sigel, H. Sigel, R. K. O. Sigel, *Structural and Catalytic Roles of Metal Ions in RNA, Vol. 9* (Eds.: A. Sigel, H. Sigel), RSC, Cambridge, **2011**.

[2] D. A. Megger, J. Müller, in *Nucleic Acids with Purine- and Pyrimidine-Derived Nucleosides, Vol. 10* (Eds.: A. Sigel, H. Sigel), RSC, Cambridge, **2012**, pp. 295–317.

[3] P. Scharf, J. Müller, *ChemPlusChem* **2013**, *78*, 20–34.

[4] E. M. Nolan, S. J. Lippard, *Chem. Rev.* **2008**, *108*, 3443–3480.

[5] J. W. Liu, Z. H. Cao, Y. Lu, *Chem. Rev.* **2009**, *109*, 1948–1998.

[6] A. A. Voityuk, *J. Phys. Chem. B* **2006**, *110*, 21010–21013.

[7] S. P. Liu, S. H. Weisbrod, Z. Tang, A. Marx, E. Scheer, A. Erbe, *Angew. Chem.* **2010**, *122*, 3385–3388; *Angew. Chem. Int. Ed.* **2010**, *49*, 3313–3316.

[8] a) A. Ono, H. Togashi, *Angew. Chem.* **2004**, *116*, 4400–4402; *Angew. Chem. Int. Ed.* **2004**, *43*, 4300–4302; b) C. Chiang, C. Huang, C. Liu, H. Chang, *Anal. Chem.* **2008**, *80*, 3716–3721; c) D. S. Chan, H. Lee, C. Che, C. Leung, D. Ma, *Chem. Commun.* **2009**, 7479–7481; B. Man, D. Chan, H. Yang, S. Ang, F. Yang, S. Yan, C. Ho, P. Wu, C. Che, C. Leung, D. Ma, *Chem. Commun.* **2010**, *46*, 8534–8536.

[9] K. Tanaka, M. Shionoya, *J. Org. Chem.* **1999**, *64*, 5002–5003.

[10] G. H. Clever, M. Shionoya, *Alternative DNA Base Pairing through Metal Coordination*, Springer, Netherlands, **2012**.

[11] D. A. Megger, C. F. Guerra, F. M. Bickelhaupt, J. Müller, *J. Inorg. Biochem.* **2011**, *105*, 1398–1404.

[12] J. Šponer, M. Sabat, J. V. Burda, J. Leszczynski, P. Hobza, B. Lippert, *J. Biol. Inorg. Chem.* **1999**, *4*, 537–545.

[13] S. Johannsen, N. Megger, D. Bohme, R. K. O. Sigel, J. Müller, *Nat. Chem.* **2010**, *2*, 229–234.

[14] K. Petrovec, B. J. Ravoo, J. Müller, *Chem. Commun.* **2012**, *48*, 11844–11846.

[15] Y. Tanaka, S. Oda, H. Yamaguchi, Y. Kondo, C. Kojima, A. Ono, *J. Am. Chem. Soc.* **2007**, *129*, 244–245.

[16] T. Uchiyama, T. Miura, H. Takeuchi, T. Dairaku, T. Komuro, T. Kawamura, Y. Kondo, L. Benda, V. Sychrovsky, P. Bour, I. Okamoto, A. Ono, Y. Tanaka, *Nucleic Acids Res.* **2012**, *40*, 5766–5774.

[17] L. Benda, M. Straka, V. Sychrovský, P. Bouř, Y. Tanaka, *J. Phys. Chem. A* **2012**, *116*, 8313–8320.

[18] H. Yamaguchi, J. Šebera, J. Kondo, S. Oda, T. Komuro, T. Kawamura, T. Daraku, Y. Kondo, I. Okamoto, A. Ono, K. Furuita, J. V. Burda, C. Kojima, V. Sychrovsky, Y. Tanaka, unpublished results.

[19] H. Torigoe, A. Ono, T. Kozasa, *Chem. Eur. J.* **2010**, *16*, 13218–13225.

[20] a) P. Pyykkö, *Chem. Rev.* **1997**, *97*, 597–636; b) P. Pyykkö, M. Straka, *Phys. Chem. Chem. Phys.* **2000**, *2*, 2489–2493; c) P. Pyykkö, M. Straka, T. Tamm, *Phys. Chem. Chem. Phys.* **1999**, *1*, 3441–3444.

[21] L. Benda, M. Straka, Y. Tanaka, V. Sychrovský, *Phys. Chem. Chem. Phys.* **2011**, *13*, 100–103.

[22] D. A. Megger, C. F. Guerra, J. Hoffmann, B. Brutschy, F. M. Bickelhaupt, J. Müller, *Chem. Eur. J.* **2011**, *17*, 6533–6544.

[23] T. Vreven, K. S. Byun, I. Komaromi, S. Dapprich, J. A. Montgomery, K. Morokuma, M. J. Frisch, *J. Chem. Theory Comput.* **2006**, *2*, 815–826.

[24] A. D. Becke, *J. Chem. Phys.* **1993**, *98*, 5648–5652.

[25] W. J. Hehre, L. Radom, P. V. R. Schleyer, J. A. Pople, *Ab initio Molecular Orbital Theory*, Wiley, New York, **1986**.

[26] a) D. Andrae, U. Haussermann, M. Dolg, H. Stoll, H. Preuss, *Theor. Chim. Acta* **1990**, *77*, 123–141; b) P. J. Hay, W. R. Wadt, *J. Chem. Phys.* **1985**, *82*, 270–283.

[27] M. Cossi, G. Scalmani, N. Rega, V. Barone, *J. Chem. Phys.* **2002**, *117*, 43–54.

[28] A. Schäfer, H. Horn, R. Ahlrichs, *J. Chem. Phys.* **1992**, *97*, 2571–2577.

[29] K. Eichkorn, F. Weigend, O. Treutler, R. Ahlrichs, *Theor. Chem. Acc.* **1997**, *97*, 119–124.

[30] A. Klamt, G. Schuurmann, *J. Chem. Soc. Perkin Trans. 2* **1993**, 799–805.

[31] Gaussian 09, Revision A.02, M. J. Frisch, G. W. Trucks, H. B. Schlegel, G. E. Scuseria, M. A. Robb, J. R. Cheeseman, G. Scalmani, V. Barone, B. Mennucci, G. A. Petersson, H. Nakatsuji, M. Caricato, X. Li, H. P. Hratchian, A. F. Izmaylov, J. Bloino, G. Zheng, J. L. Sonnenberg, M. Hada, M. Ehara, K. Toyota, R. Fukuda, J. Hasegawa, M. Ishida, T. Nakajima, Y. Honda, O. Kitao, H. Nakai, T. Vreven, J. A. Montgomery, Jr., J. E. Peralta, F. Ogliaro, M. Bearpark, J. J. Heyd, E. Brothers, K. N. Kudin, V. N. Staroverov, R. Kobayashi, J. Normand, K. Raghavachari, A. Rendell, J. C. Burant, S. S. Iyengar, J. Tomasi, M. Cossi, N. Rega, J. M. Millam, M. Klene, J. E. Knox,

J. B. Cross, V. Bakken, C. Adamo, J. Jaramillo, R. Gomperts, R. E. Stratmann, O. Yazyev, A. J. Austin, R. Cammi, C. Pomelli, J. W. Ochterski, R. L. Martin, K. Morokuma, V. G. Zakrzewski, G. A. Voth, P. Salvador, J. J. Dannenberg, S. Dapprich, A. D. Daniels, Ö. Farkas, J. B. Foresman, J. V. Ortiz, J. Cioslowski, D. J. Fox, Gaussian, Inc. Wallingford CT, **2009**.

[32] R. Ahlrichs, M. Bar, M. Häser, H. Horn, C. Kolmel, *Chem. Phys. Lett.* **1989**, *162*, 165–169.

[33] A. T. Afaneh, G. Schreckenbach, F. Y. Wang, *Theor. Chem. Acc.* **2012**, *131*, 1174–1190.

[34] S. Sjoberg, *Acta Chem. Scand. Acta Chem. Scand.* **1977**, *31*, 705–717.

[35] P. Soldán, E. P. F. Lee, T. G. Wright, *J. Phys. Chem. A* **2002**, *106*, 8619–8626.

[36] Y. Miyake, H. Togashi, M. Tashiro, H. Yamaguchi, S. Oda, M. Kudo, Y. Tanaka, Y. Kondo, R. Sawa, T. Fujimoto, T. Machinami, A. Ono, *J. Am. Chem. Soc.* **2006**, *128*, 2172–2173.

[37] N. J. Kim, *Bull. Korean Chem. Soc.* **2006**, *27*, 1009–1014.

[38] J. Burda, J. S. Gutiérrez-Oliva, S. Politzer, P. Toro-Labbé, unpublished results.

[39] H. Torigoe, Y. Miyakawa, A. Ono, T. Kozasa, *Thermochim. Acta* **2012**, *532*, 28–35.